# Deformation Behaviors of Geogrid-reinforced Soil Walls: Single-Tier versus Two-Tier Walls

**Pham Ngoc Thach**
Ho Chi Minh City University of Transport, Ho Chi Minh City, Vietnam
thach.pham@ut.edu.vn (corresponding author)

**Hoang Khac Tuan**
Boydens Vietnam Part of Sweco, Ho Chi Minh City, Vietnam
tuan.hoang@sweco.vn

*Received: 13 February 2025 | Revised: 5 March 2025 and 13 March 2025 | Accepted: 17 March 2025*

 *DOI: https://doi.org/10.48084/etasr.10568*

## ABSTRACT

**Geogrid Reinforced Soil (GRS) walls are used in the construction of bridge abutments, highways, and areas with raised elevations. Regarding conventional GRS walls, the wall facing is usually designed in a single-tier configuration. However, when a large wall height is required, the facing can be designed in a multi-tier configuration. Multi-tiered walls exhibit a more complex behavior than single-tier walls due to interactions between the upper and lower tiers. To gain further understanding of these differences between the two types of GRS walls, a numerical study was conducted to compare the self-weight induced deformation of a single-tier GRS wall to this of a two-tier GRS wall. The deformation behaviors include the horizontal displacement of wall facing, the horizontal displacement of backfill surface, and the tensile strain of geogrid layers.**

***Keywords-geogrid; reinforced soil wall; deformation behavior; finite element analysis***

## I. INTRODUCTION

GRS walls consist of facing, backfill soil, geogrid layers, and subgrade soil. The inclusion of geogrid layers in the backfill soil leads to enhanced compressive and tensile strength of the reinforced backfill material. Taking advantage of this characteristic, GRS walls have been increasingly used for bridge abutments, highways, and areas with raised elevations to support bridge approaches [1-3]. For systems with larger height the wall facing can be designed in a multi-tier configuration. Numerical studies have revealed that multi-tiered walls exhibit more complex behaviors than single-tier walls due to the interaction between the upper and lower tiers [4, 5]. In this study, the finite element method is utilized to simulate the self-weight induced behaviors of an 8.4 m high GRS wall with two cases of tier configurations: single-tier wall and two-tier wall. The study aims to compare the deformation behaviors of the two cases, specifically, the horizontal displacement of wall facing, the horizontal displacement of backfill surface, and the tensile strain of geogrid layers.

## II. GRS WALL DESCRIPTION

The cross-section of the single-tier and two-tier GRS walls utilized in this study is illustrated in Figure 1. The input data for the single-tier wall is an 8.4 m high retaining wall segment of the Myphuoc-Tanvan bridge approach road in Binh Duong province of Vietnam.

It is assumed that the two-tier wall differs from the single-tier wall solely in the tier configuration. The walls have a total height ($H$) of 8.4 m. For the two-tier wall, shown in Figure 1b, it is assumed that the heights of the lower and upper tier, $H_1$ and $H_2$, respectively, are 4.2 m. If the offset distance ($D$) between the two tiers is too small, a two-tier wall will behave like a single-tier wall. Therefore, $D$ is assumed to be 2.1 m to ensure that complex interactions between the two tiers take place. This $D$ value is consistent with the design range $H/20 < D < H_2 \tan(90 - \varphi)$, as proposed by FHWA, where $\varphi$ is the internal friction angle of the backfill soil [6]. The wall facing consists of segmental concrete blocks measuring 0.2 m x 1.2 m. The wall base is placed on a concrete footing with dimensions of 0.5 m x 0.3 m.

The backfill material is cohesionless and reinforced with layers of Tensar RE570 geogrids. The geogrid layers are spaced 0.6 m vertically and the ends of the geogrid layers are bolted to the wall facing. For the single-tier wall, the geogrid layers are 7 m long. Due to the focus of this study on the effect of tiering rather than the impact of geogrid length on the wall behaviors, it is assumed that the geogrid layers of the two-tier wall were also 7 m long, similar to the single-tier wall. This length is approximately 0.83 $H$, which exceeds the minimum geogrid lengths of 0.35 $H$ and 0.6 $H$ for the upper tier and the lower tier, respectively, as proposed by the FHWA [6]. Table I summarizes the material properties.

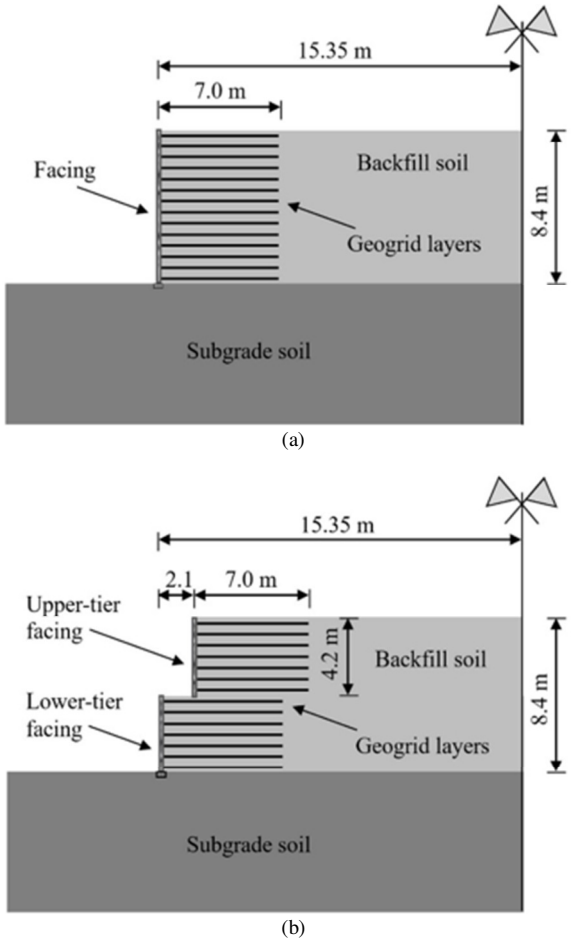


Fig. 1. GRS walls for: (a) single-tier and (b) two-tier wall.

TABLE I. MATERIAL PROPERTIES

| Component | Parameter | Value | Unit |
|---|---|---|---|
| Concrete block | Elastic modulus | 28750 | MPa |
| | Poisson's ratio | 0.2 | - |
| | Unit weight | 24 | kN/m$^3$ |
| Geogrid | Elastic modulus | 2153 | MPa |
| | Poisson's ratio | 0.3 | - |
| | Tesile strength | 118.4 | kN/m |
| | Yielding strain | 0.1 | - |
| Backfill soil | Elastic modulus | 50 | MPa |
| | Poisson's ratio | 0.35 | - |
| | Unit weight | 18 | kN/m$^3$ |
| | Cohesion | 0 | kPa |
| | Internal friction angle | 30 | ° |
| | Dilatancy angle | 0 | ° |
| Subgrade soil | Elastic modulus | 40 | MPa |
| | Poisson's ratio | 0.35 | - |
| | Unit weight | 17.5 | kN/m$^3$ |
| | Cohesion | 0 | kPa |
| | Internal friction angle | 30 | ° |
| | Dilatancy angle | 0 | ° |

## III. NUMERICAL SIMULATION METHOD

### A. Simulation Method

The finite element program Abaqus is used for numerical simulation [7]. Figure 2 presents the plane strain Finite Element Model (FEM) of the single-tier and two-tier walls. The backfill, subgrade soil and facing blocks were meshed with CPE4R elements, which are plane strain 4-node quadrilateral elements with reduced integration. The geogrid reinforcement layers were meshed with T2D2 elements, which are 2-node truss elements whose compressive stiffness was not activated.

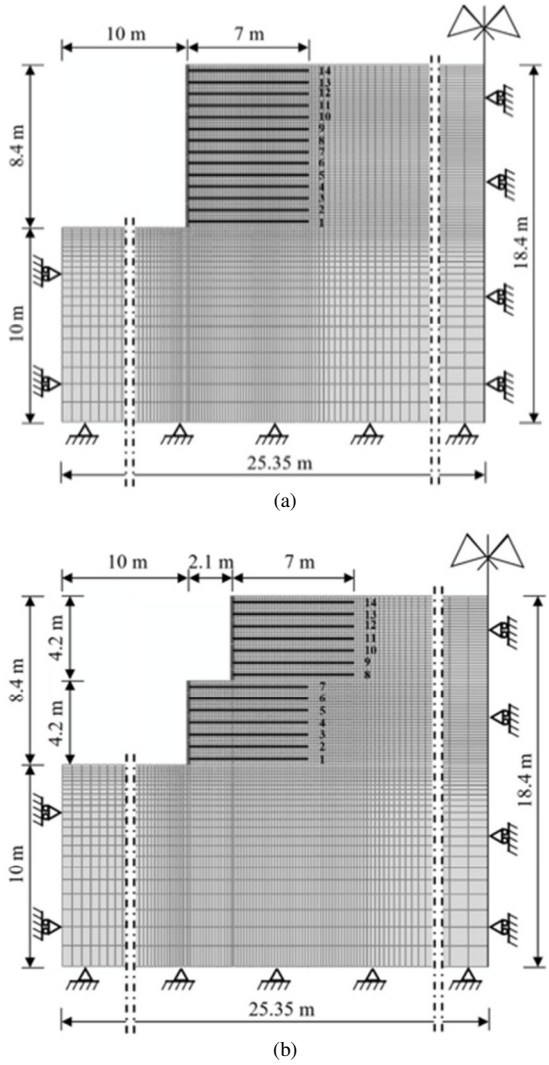


Fig. 2. FEM for: (a) single-tier and (b) two-tier wall.

The backfill soil interacts with the facing blocks and the blocks also interact with each other at their contact surfaces. These contact interactions were modeled using surface-to-surface contact elements [7]. Their frictional behavior is characterized by the Coulomb friction model with a friction coefficient ($\mu$) equal to the tangent of the friction angle ($\delta$) between the contact materials. Based on [6], $\delta$ is assumed to be

equal to 2/3 of $\varphi$ for the contact between the backfill soil and facing blocks. For a $\varphi$ value of 20 °, the corresponding $\mu$ is 0.36. According to [8], $\mu$ is assumed to be 0.3 regarding the contact between the facing blocks, which deform together but the relative slip between them is almost negligible [9]. It is therefore assumed that there is no slip between the geogrid layers and backfill soil, and so the nodes of T2D2 reinforcement elements were connected tightly to the nodes of CPE4R elements.

The nonlinear behavior of the backfill and subgrade soils is represented by the Mohr-Coulomb soil model with the following material parameters: elastic modulus, Poisson's ratio, $\varphi$, cohesion, and dilatation angle ($\psi$), with their values being summarized in Table I. It should be noted that $\psi$ is approximated by the expression $\psi = \varphi - 30°$ for cohesionless soils [10]. In Table I, the backfill and subgrade soils' $\varphi$ value is 30 ° and the corresponding $\psi$ values is 0 °. Furthermore, the facing blocks are assumed to behave as a linear elastic material. The axial tensile behavior of the geogrid layers is represented by the ideal elastic-plastic model with the following material parameters: elastic modulus, Poisson's ratio, yield strain, and tensile strength, with their values also being listed in Table I. The deformation of the soil retaining systems was simulated through a series of construction steps, each representing the placement of a thin layer of backfill, geogrid, and facing blocks. The self-weight of these material components is the sole loading source that causes the soil retaining system to deform.

### *B. Validation*

The numerical simulation method is verified through the experimental measurement data from [11]. The experimental system is a 6 m high GRS wall. The width of the backfill is 5 m. The wall facing was constructed using precast concrete blocks with dimensions of 0.45 m x 0.55 m for the wall body and 0.50 m x 0.35 m for the wall base. There are eleven geogrid layers in which 3.5 m long geogrid layers are arranged alternately with 1.0 m long geogrid layers. Table II outlines the material property parameters.

TABLE II. MATERIAL PROPERTIES OF EXPERIMENTAL SYSTEM

| Component | Parameter | Value | Unit |
|---|---|---|---|
| Concrete block | Elastic modulus | 2 × 106 | kPa |
| | Poisson's ratio | 0.2 | |
| | Unit weight | 23 | kN/m3 |
| Geogrid | Elastic modulus | 1.57 × 106 | kPa |
| | Poisson's ratio | 0.3 | |
| | Tesile strength | 54.6 | kN/m |
| | Yielding strain | 0.12 | |
| Backfill soil | Elastic modulus | 104 | kPa |
| | Poisson's ratio | 0.42 | |
| | Unit weight | 16 | kN/m3 |
| | Cohesion | 0 | kPa |
| | Internal friction angle | 45 | ° |
| | Dilatancy angle | 15 | ° |

Additionally, measurement devices are arranged on the wall facing and geogrid layers to measure the horizontal displacement of the wall facing and the axial deformation of the reinforcement layers. Figure 3 illustrates the FEM, which was built using the simulation method presented in the preceding section.

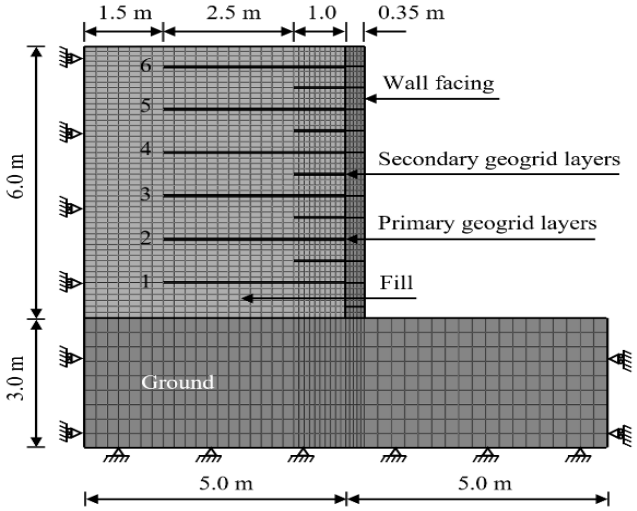


Fig. 3. FEM of the verification problem.

Furthermore, Figure 4 presents the horizontal displacement of the facing against the wall height. The horizontal displacement of the facing exhibits a similar pattern between the FEM and the experimental results. Specifically, the displacement reaches a peak value around the mid-height of the wall, while the displacements are minimized at the bottom and top of the wall.

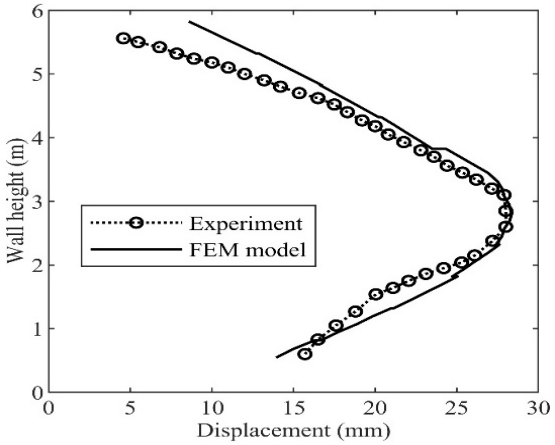


Fig. 4. Horizontal displacement of the facing.

In addition, Figure 5 portrays the tensile strain of the primary geogrid layers against the distance from the wall. In specific, maximum strain values are observed closer to the wall, while strain decreases as the distance from the wall increases. The numerical simulation and experimental measurements are consistent.

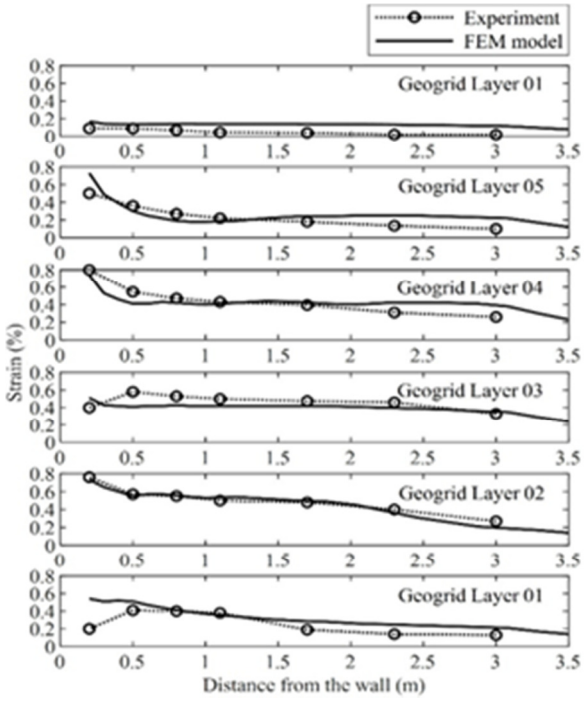


Fig. 5. Tensile strain of the primary geogrid layers.

## IV. RESULTS AND DISCUSSION

### A. *Contour of Horizontal Displacement*

Figure 6 demonstrates the horizontal displacement contours of single-tier and two-tier walls. In both cases it is evident that the facing and the backfill underwent significant horizontal displacements, as indicated by the wedge-shaped area bounded by the green strip. For the single-tier wall, large displacements appeared mid-height. In contrast, for the two-tier wall, large displacements are shifted to the mid-height of the lower tier.

### B. *Horizontal Displacement of the Facing*

Figure 7 shows the horizontal displacement of the facing for single-tier and two-tier walls. For the single-tier, the displacement was 25.6 mm at the facing top and reached a maximum value of 38.3 mm at 3.6 m from the facing bottom. This maximum value is equal to 0.0046 *H*, which is close to the safety limit of 0.005 *H*, commonly assumed in Vietnam practice. The two-tier wall significantly reduced the horizontal displacement of the facing in comparison with the single-tier. Specifically, at the facing top, the displacement decreased from 25.6 mm to 22.5 mm at 3.6 m from the facing bottom, the displacement decreased from 38.3 mm to 26.4 mm and the maximum value decreased from 38.3 mm to 31.7 mm. The displacement reduction is a consequence of the tier configuration. The complex interaction between the upper-tier facing, lower-tier facing, reinforcement layers, and backfill soil under the influence of their own weight resulted in a reduction of the earth pressure on the facing, leading in turn to a decrease in the horizontal displacement of the facing.

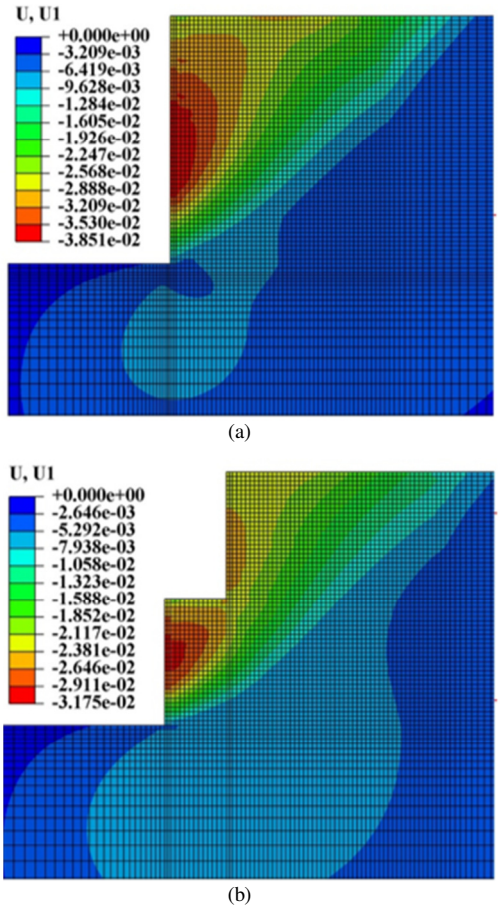


Fig. 6. Contour of horizontal displacement for: (a) single-tier and (b) two-tier wall.

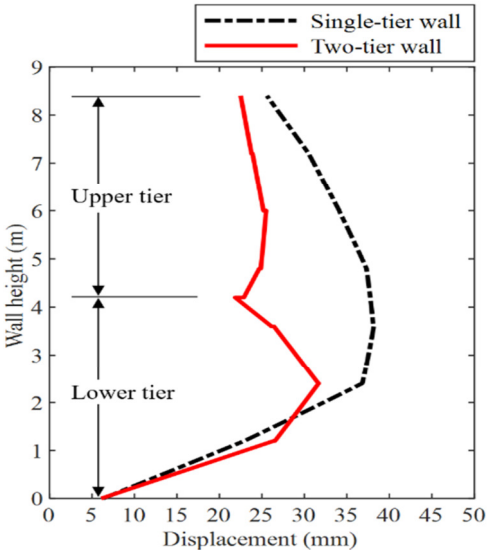


Fig. 7. Horizontal displacement of the facing for single and two-tier walls.

For the two-tier wall, the displacement differences between the top, middle, and bottom are quite small. Specifically, the difference between the maximum displacement and the

displacement at the bottom is 2.6 mm. Meanwhile, at the lower tier facing, this difference is 25.6 mm, that is, larger than the one of the upper tier facing. This observation implies that the use of the two-tier configuration reduced the influence of the backfill self-weight on the horizontal displacement of the upper-tier facing. These findings suggest that for GRS retaining wall projects similar to the Myphuoc-Tanvan, reducing the facing thickness or utilizing more cost-effective materials for the upper tier facing can reduce project cost.

### *C. Horizontal Displacement of the Backfill Surface*

Figure 8 presents the horizontal displacement of the backfill surface. For the single-tier wall, the displacement is large at points near the facing with a maximum value of 27.5 mm at 3.2 m from the facing. The displacement decreases as the distance from the facing increases. These findings indicate an irregular distribution of the horizontal displacement of the backfill surface. Since the backfill served as a subgrade of the road pavement the displacement of the backfill surface could lead to pavement surface cracking, thus affecting the long-term serviceability and maintenance costs.

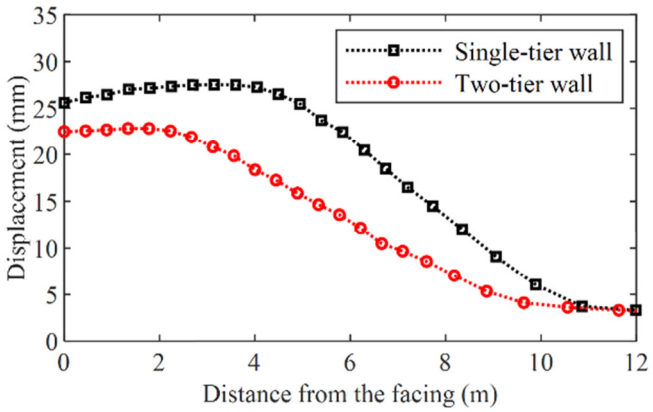


Fig. 8. Horizontal displacement of the backfill surface for single and two-tier walls.

The two-tier wall reduced the horizontal displacement of the backfill surface when comparing both cases. Specifically, at 3.2 m from the facing, the displacement was reduced from 27.5 mm to 20.6 mm. The maximum displacement was reduced from 27.5 mm to 22.8 mm suggesting that the reduction in the horizontal displacement would benefit the long-term serviceability of the road pavement constructed on the backfill.

### *D. Axial Tensile Strain of Geogrid Layers*

Figure 9 illustrates the axial tensile strain of 14 geogrid layers, numbered from 1 to 14 in Figure 2. The geogrid layers in the two-tier wall presented smaller strains in general than those in the single-tier wall. The geogrid strain adjacent to the wall facing is presented in Figure 10, and the maximum geogrid strain in each geogrid layer is depicted in Figure 11.

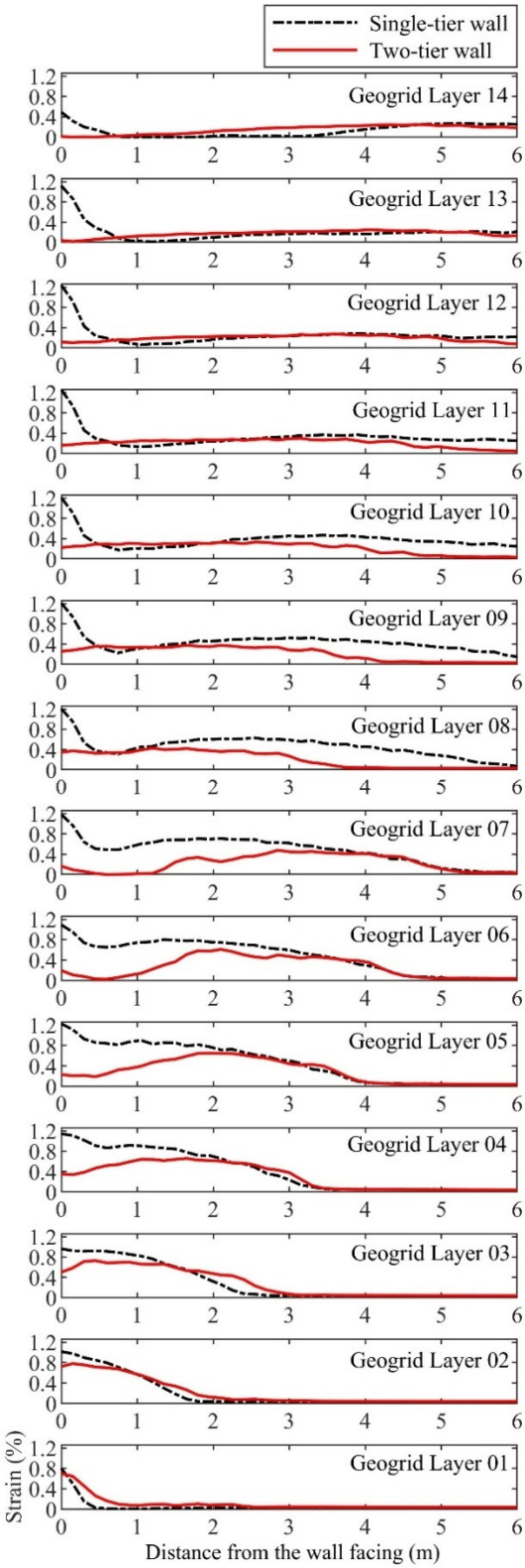


Fig. 9. Axial tensile strain of geogrid layers.

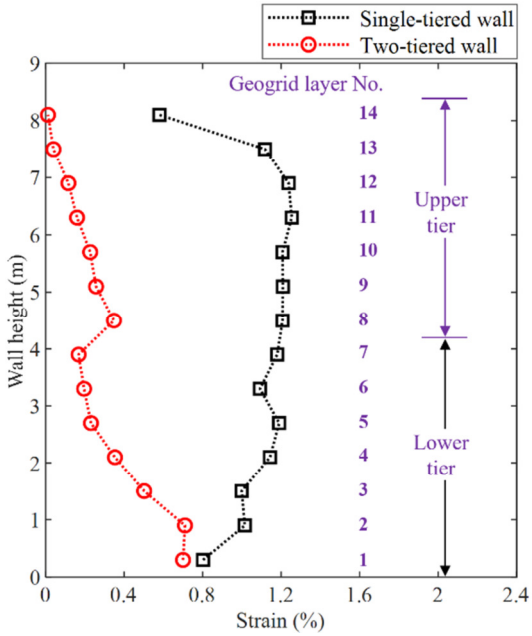


Fig. 10. Geogrid strain at vicinity of the wall facing.

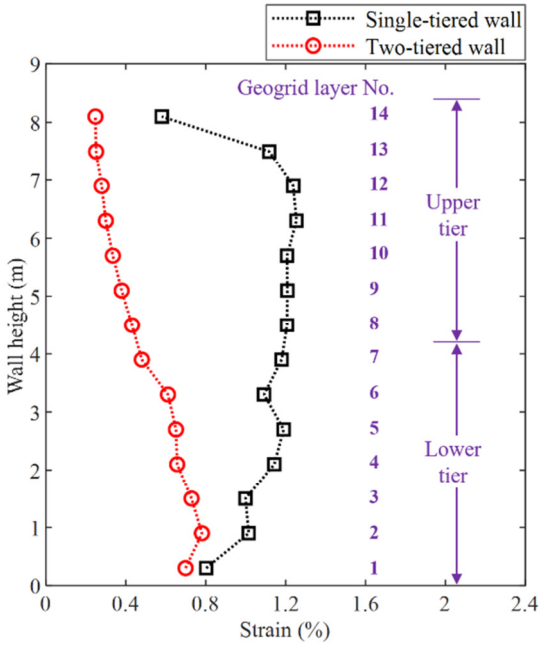


Fig. 11. Maximum geogrid strain.

As evidenced in Figure 10, the geogrid layers proposed a relatively large strain in the vicinity of the wall facing, with the largest value of 0.0125 being obtained in the geogrid layer 11, regarding the single-tier wall. Comparing both wall cases it is observed that the two-tier wall significantly reduced the geogrid strain, especially in the geogrid layers 3-14. Additionally, as illustrated in Figure 11, the two-tier wall reduced the maximum geogrid strain from 0.0125 to 0.0078. Moreover, the upper tier had a maximum strain of 0.0043, which was significantly smaller than the value of 0.0078 of the lower tier. The results indicate that the two-tier wall significantly reduced the strain in geogrid layers. The upper tier geogrid layers experienced a definite strain reduction compared to the lower tier geogrid layers.

## V. CONCLUSIONS

The displacement at the facing top of the two-tier wall is reduced from 25.6 mm to 22.5 mm and the maximum displacement from 38.3 mm to 31.7 mm in comparison with the single-tier wall. Moreover, the relative displacements between the top, middle, and bottom of the upper-tier facing are relatively small. These findings suggest that for Geogrid Reinforced Soil (GRS) retaining wall projects similar to the Myphuoc-Tanvan, reducing the facing thickness or utilizing more cost-effective materials for the upper tier facing can decrease project costs.

The horizontal displacement of the backfill surface for the single-tier wall is higher near the facing and lower further away. Since the backfill served as a subgrade for road pavement, this irregular and significant horizontal displacement of the backfill surface could lead to pavement surface cracking, thus affecting the long-term serviceability. Furthermore, regarding the two-tier wall, the horizontal displacement is reduced, with the maximum value ranging from 27.5 mm to 22.8 mm. This reduction can benefit the long-term serviceability of the road pavement constructed on the backfill.

The geogrid layers had a significant tensile strain in the vicinity of the facing regarding the single-tier wall case. On the contrary, the two-tier wall system exhibited reduced tensile strain in the geogrid layers, with the largest geogrid strain having been reduced from 0.0125 to 0.0078. The strain reduction is more obvious in the upper-tier geogrid layers than in the lower-tier geogrid layers.

The present study examined a limited number of cases. The results and conclusions contribute to the understanding of how a two-tier wall behaves differently from a single-tier wall. The former can serve as a reference for similar GRS wall projects, where the performance of a two-tier RGS wall design needs to be evaluated.

## REFERENCES

[1] J. Evans, D. Ruffing, and D. Elton, *Fundamentals of Ground Improvement Engineering*, 1st ed. London, UK: CRC Press, 2021.

[2] M. Touahmia, "Performance of Geosynthetic-Reinforced Soils Under Static and Cyclic Loading," *Engineering, Technology & Applied Science Research*, vol. 7, no. 2, pp. 1523–1527, Apr. 2017, https://doi.org/10.48084/etasr.1035.

[3] K. Malekmohammadi and I. P. Damians, "A Bibliometric Review of Reinforced Soil Wall Research Topics," *International Journal of Geosynthetics and Ground Engineering*, vol. 10, no. 3, May 2024, Art. no. 42, https://doi.org/10.1007/s40891-024-00537-3.

[4] F. Ali, S. Benmebarek, and M. Djabri, "Numerical investigations of GRS wall performance with tiered configurations," *Studies in Enfineering and Exact Sciences*, vol. 5, no. 2, Jul. 2024, Art. no. e5857, https://doi.org/10.54021/seesv5n2-031.

[5] F. Zhang, B. Ge, D. Leshchinsky, S. Shu, and Y. Gao, "Effects of Multitiered Configuration on the Internal Stability of GRS Walls," *Journal of Geotechnical and Geoenvironmental Engineering*, vol. 149, no. 12, Dec. 2023, Art. no. 04023122, https://doi.org/10.1061/JGGEFK.GTENG-11723.

[6] *LRFD Bridge Design Specifications*, American Association of State Highway and Transportation Officials, Washington DC, USA, 2012.

[7] *Abaqus*, Dassault Systèmes, Available: https://www.3ds.com/products/simulia/abaqus.

[8] H. I. Ling and H. Liu, "Deformation analysis of reinforced soil retaining walls—simplistic versus sophisticated finite element analyses," *Acta Geotechnica*, vol. 4, no. 3, pp. 203–213, Sep. 2009, https://doi.org/10.1007/s11440-009-0091-6.

[9] C. Yoo, "Serviceability state deformation behaviour of two-tiered geosynthetic reinforced soil walls," *Geosynthetics International*, vol. 25, no. 1, pp. 12–25, Feb. 2018, https://doi.org/10.1680/jgein.17.00030.

[10] M. D. Bolton, "The strength and dilatancy of sands," *Géotechnique*, vol. 36, no. 1, pp. 65–78, Mar. 1986, https://doi.org/10.1680/geot.1986.36.1.65.

[11] H. I. Ling, C. P. Cardany, L.-X. Sun, and H. Hashimoto, "Finite Element Study of a Geosynthetic-Reinforced Soil Retaining Wall With Concrete-Block Facing," *Geosynthetics International*, vol. 7, no. 3, pp. 163–188, Jan. 2000, https://doi.org/10.1680/gein.7.0171.